Beam Instabilities in Linear Machines: Space Charge Effects

M. Ferrario
Frascati National Laboratory, National Institute for Nuclear Physics, Rome, Italy

Abstract

In this paper we introduce, from basic principles, the main concepts of beam focusing and transport in modern accelerators using the beam envelope equation as a convenient mathematical tool. Matching conditions suitable for preserving beam quality are derived from the model for significant beam dynamics regimes.

Keywords

Beam matching; rms emittance; laminar beam; space charge effects; rms envelope equations.

1   Introduction

Light sources based on high-gain free electron lasers or future high-energy linear colliders require the production, acceleration, and transport up to the interaction point of low divergence, high charge-density electron bunches [1]. Many effects contribute in general to degradation of the final beam quality, including chromatic effects, wake fields, emission of coherent radiation, and accelerator misalignments. Space charge effects and mismatch with focusing and accelerating devices typically contribute to emittance degradation of high charge-density beams [2]; hence, control of beam transport and acceleration is the leading edge for high-quality beam production.

Space charge effects represent a very critical issue and a fundamental challenge for high-quality beam production and its applications. Without proper matching, significant emittance growth may occur when the beam is propagating through different stages and components, owing to the large differences of transverse focusing strength. This unwanted effect is even more serious in the presence of finite energy spread.

In this paper we introduce, from basic principles, the main concepts of beam focusing and transport in modern accelerators using the beam envelope equation as a convenient mathematical tool. Matching conditions suitable for preserving beam quality are derived from the model for significant beam dynamics regimes. A more detailed discussion of the previous topics can be found in the many classical textbooks on this subject, as listed in Refs. [3–6].

2   Laminar and non-laminar beams

An ideal high-charge particle beam has orbits that flow in layers that never intersect, as occurs in a laminar fluid. Such a beam is often called a laminar beam. More precisely, a laminar beam satisfies the following two conditions [6]:

i)   all particles at a given position have identical transverse velocities. On the contrary, the orbits of two particles that start at the same position could separate and later cross each other.

ii)   assuming that the beam propagates along the z axis, the magnitudes of the slopes of the trajectories in the transverse directions x and y, given by $x'(z) = \mathrm{d}x/\mathrm{d}z$ and $y'(z) = \mathrm{d}y/\mathrm{d}z$, are linearly proportional to the displacement from the z axis of beam propagation.

Trajectories of interest in beam physics are always confined to the inside of small, near-axis regions, and the transverse momentum is much smaller than the longitudinal momentum, $p_{x,y} \ll p_z \approx p$. As a consequence, it is convenient in most cases to use the small angle, or *paraxial*, approximation, which allows us to write the useful approximate expressions $x' = p_x/p_z \approx p_x/p$ and $y' = p_y/p_z \approx p_x/p$.

To help understand the features and advantages of a laminar beam propagation, the following figures compare the typical behaviour of a laminar and a non-laminar (or thermal) beam.

Figure 1 illustrates an example of orbit evolution of a laminar mono-energetic beam with half width x_0 along a simple beam line with an ideal focusing element (solenoid, magnetic quadrupoles, or electrostatic transverse fields are usually adopted to this end), represented by a thin lens located at the longitudinal coordinate $z = 0$. In an ideal lens, focusing (defocusing) forces are linearly proportional to the displacement from the symmetry axis z, so that the lens maintains the laminar flow of the beam.
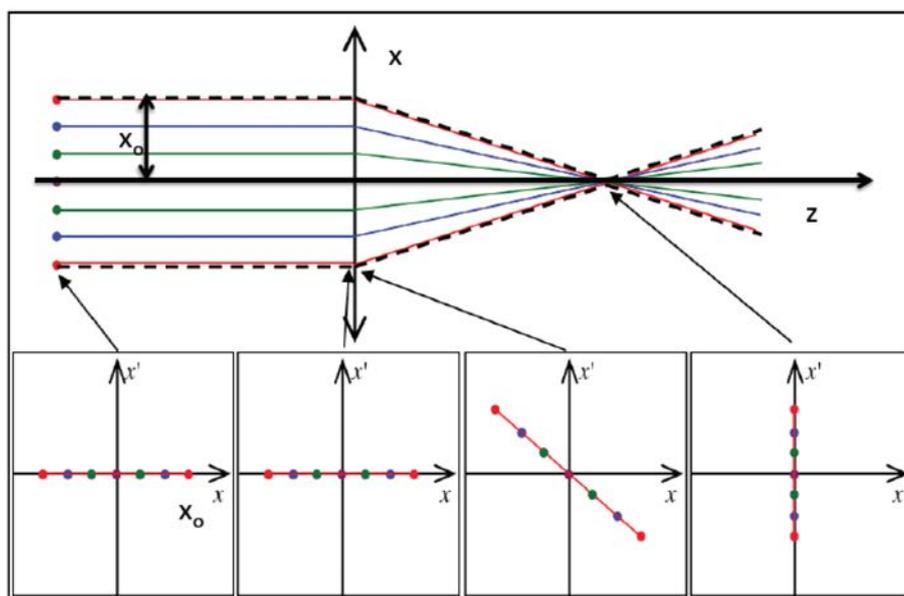

Fig. 1: Particle trajectories and phase space evolution of a laminar beam [7]

The beam shown in Fig. 1 starts propagating completely parallel to the symmetry axis z; in this particular case, the particles all have zero transverse velocity. There are no orbits that cross each other in such a beam. Ignoring collisions and inner forces, such as coulomb forces, such a parallel beam could propagate an infinite distance with no change in its transverse width. When the beam crosses the ideal lens, it is transformed into a converging laminar beam. Because the transverse velocities after the linear lens are proportional to the displacement off-axis, particle orbits define similar triangles that converge to a single point. After passing through the singularity at the focal point, the particles follow diverging orbits. We can always transform a diverging (or converging) beam into a parallel beam by using a lens of the proper focal length, as can be seen by reversing the propagation axis of Fig. 1.

The small boxes in the lower part of the figure depict the particle distributions in the trace space (x, x'), equivalent to the canonical phase space $(x, p_x \approx x'p)$ when p is constant, i.e. without beam acceleration. The phase space area occupied by an ideal laminar beam is a straight segment of zero thickness. As can be easily verified, the condition that the particle distribution has zero thickness proceeds from condition 1; the segment straightness is a consequence of condition 2. The distribution of a laminar beam propagating through a transport system with ideal linear focusing elements is thus a straight segment with variable slope.

Particles in a non-laminar beam have a random distribution of transverse velocities at the same location and a spread in directions, as shown in Fig. 2. Because of the disorder of a non-laminar beam, it is impossible to focus all particles from a location in the beam toward a common point. Lenses can

influence only the average motion of particles. Focal spot limitations are a major concern for a wide variety of applications, from electron microscopy to free electron lasers and linear colliders. The phase space plot of a non-laminar beam is no longer a straight line: the beam, as shown in the lower boxes of Fig. 2, occupies a wider area of the phase space.
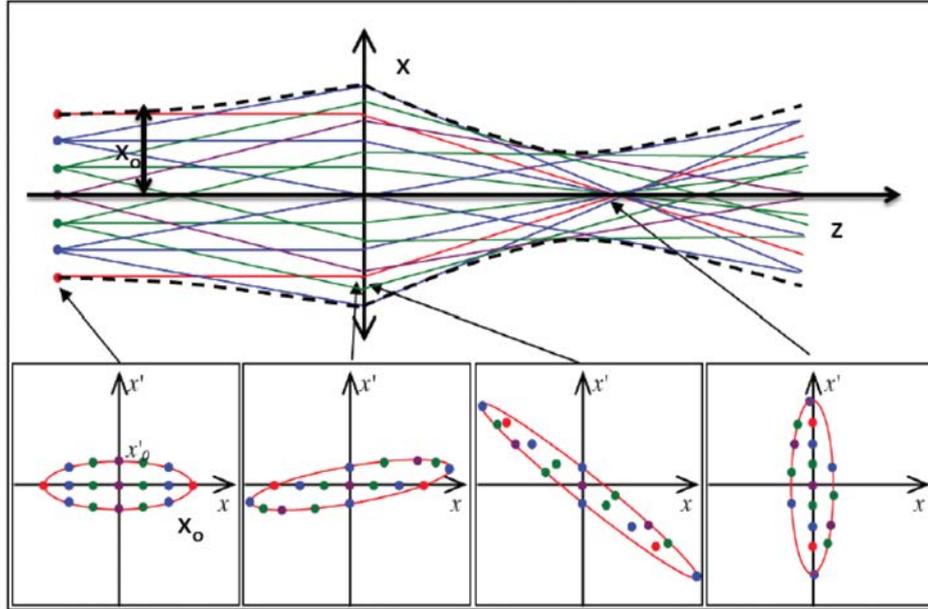

Fig. 2: Particle trajectories and phase space evolution of a non-laminar beam [7]

3   The emittance concept

The phase space surface A occupied by a beam is a convenient figure of merit for designating the quality of a beam. This quantity is the emittance ε_x and is usually represented by an ellipse that contains the whole particle distribution in the phase space (x, x'), such that $A = \pi\varepsilon_x$. An analogous definition holds for the (y, y') and (z, z') planes. The original choice of an elliptical shape comes from the fact that when linear focusing forces are applied to a beam, the trajectory of each particle in phase space lies on an ellipse, which may be called the trajectory ellipse. Being the area of the phase space, the emittance is measured in millimetres milliradians or, more often, in micrometres.

The ellipse equation is written as

$$\gamma_x x^2 + 2\alpha_x x x' + \beta_x x'^2 = \varepsilon_x \, , \tag{1}$$

where x and x' are the particle coordinates in the phase space and the coefficients $\alpha_x(z)$, $\beta_x(z)$, and $\gamma_x(z)$ are called Twiss parameters, which are related by the geometrical condition

$$\beta_x \gamma_x - \alpha_x^2 = 1 \, . \tag{2}$$

As shown in Fig. 3, the beam envelope boundary X_{max}, its derivative $(X_{max})'$ and the maximum beam divergence X'_{max}, i.e. the projection on the axes x and x' of the ellipse edges, can be expressed as a function of the ellipse parameters:

$$\begin{cases} X_{max} = \sqrt{\beta_x \varepsilon_x} \\ (X_{max})' = -\alpha\sqrt{\dfrac{\varepsilon}{\beta}} \\ X'_{max} = \sqrt{\gamma_x \varepsilon_x} \end{cases} . \tag{3}$$
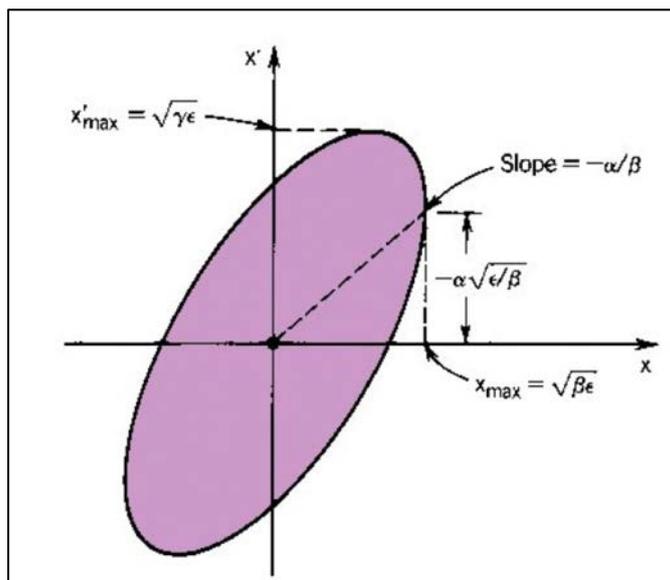
Fig. 3: Phase space distribution in a skewed elliptical boundary, showing the relationship of Twiss parameters to the ellipse geometry [6].

According to Liouville's theorem, the six-dimensional (x, p_x, y, p_y, z, p_z) phase space volume occupied by a beam is constant, provided that there are no dissipative forces, no particles lost or created, and no coulomb scattering among particles. Moreover, if the forces in the three orthogonal directions are uncoupled, Liouville's theorem also holds for each reduced phase space surface, (x, p_x), (y, p_y), (z, p_z), and hence emittance also remains constant in each plane [3].

Although the net phase space surface occupied by a beam is constant, non-linear field components can stretch and distort the particle distribution in the phase space, and the beam will lose its laminar behaviour. A realistic phase space distribution is often very different from a regular ellipse, as shown in Fig. 4.
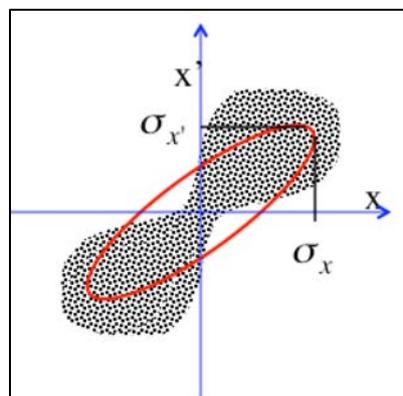

Fig. 4: Typical evolution of phase space distribution (black dots) under the effects of non-linear forces with the equivalent ellipse superimposed (red line).

We introduce, therefore, a definition of emittance that measures the beam quality rather than the phase space area. It is often more convenient to associate a statistical definition of emittance with a generic distribution function $f(x, x', z)$ in the phase space; this is the so-called *root mean square (rms) emittance*:

$$\gamma_x x^2 + 2\alpha_x x x' + \beta_x x'^2 = \varepsilon_{x,\mathrm{rms}} \ . \tag{4}$$

The rms emittance is defined such that the equivalent-ellipse projections on the x and x' axes are equal to the rms values of the distribution, implying the following conditions:

$$\begin{cases} \sigma_x = \sqrt{\beta_x \varepsilon_{x,\mathrm{rms}}} \\ \sigma_{x'} = \sqrt{\gamma_x \varepsilon_{x,\mathrm{rms}}} \end{cases} , \tag{5}$$

where

$$\begin{cases} \sigma_x^2(z) = \left\langle x^2 \right\rangle = \int\limits_{-\infty}^{+\infty} \int\limits_{-\infty}^{+\infty} x^2 f(x,x',z)\,\mathrm{d}x\mathrm{d}x' \\ \sigma_{x'}^2(z) = \left\langle x'^2 \right\rangle = \int\limits_{-\infty}^{+\infty} \int\limits_{-\infty}^{+\infty} x'^2 f(x,x',z)\,\mathrm{d}x\mathrm{d}x' \end{cases} \tag{6}$$

are the second moments of the distribution function $f(x, x', z)$. Another important quantity that accounts for the degree of (x, x') correlations is defined as

$$\sigma_{xx'}(z) = \left\langle xx' \right\rangle = \int\limits_{-\infty}^{+\infty} \int\limits_{-\infty}^{+\infty} xx' f(x,x',z)\,\mathrm{d}x\mathrm{d}x' . \tag{7}$$

From Eq. (3) it also holds that

$$\sigma_x' = \frac{\sigma_{xx'}}{\sigma_x} = -\alpha_x \sqrt{\frac{\varepsilon_{x,\mathrm{rms}}}{\beta_x}} ;$$

see also Eq. (16), which allows us to link the correlation moment Eq. (7) to the Twiss parameter as

$$\sigma_{xx'} = -\alpha_x \varepsilon_{x,\mathrm{rms}} . \tag{8}$$

One can easily see from Eqs. (3) and (5) that

$$\alpha_x = -\frac{1}{2}\frac{\mathrm{d}\beta_x}{\mathrm{d}z}$$

also holds.

By substituting the Twiss parameter defined by Eqs. (5) and (8) into condition 2 we obtain [5]

$$\frac{\sigma_{x'}^2}{\varepsilon_{x,\mathrm{rms}}}\frac{\sigma_x^2}{\varepsilon_{x,\mathrm{rms}}} - \left(\frac{\sigma_{xx'}}{\varepsilon_{x,\mathrm{rms}}}\right) = 1 . \tag{9}$$

Reordering the terms in Eq. (8) we obtain the definition of *rms emittance* in terms of the second moments of the distribution:

$$\varepsilon_{\mathrm{rms}} = \sqrt{\sigma_x^2 \sigma_{x'}^2 - \sigma_{xx'}^2} = \sqrt{\left(\left\langle x^2 \right\rangle\left\langle x'^2 \right\rangle - \left\langle xx' \right\rangle^2\right)} , \tag{10}$$

where we omit, from now on, the subscript x in the emittance notation: $\varepsilon_{\mathrm{rms}} = \varepsilon_{x,\mathrm{rms}}$. The rms emittance tells us some important information about phase space distributions under the effect of linear or non-linear forces acting on the beam. Consider, for example, an idealized particle distribution in phase space that lies on some line that passes through the origin, as illustrated in Fig. 5.
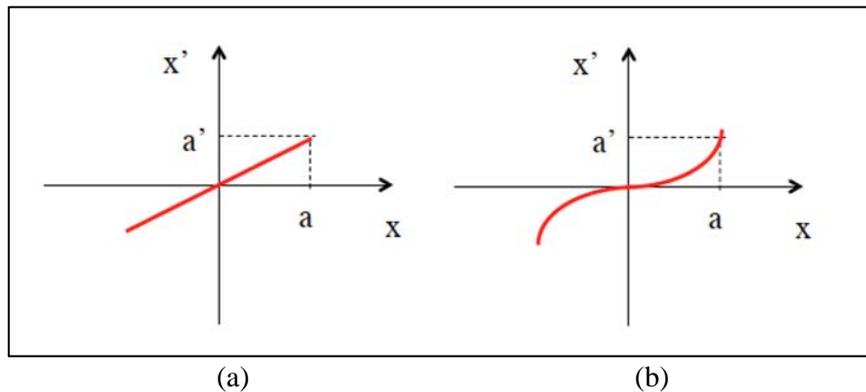
(a)   (b)

Fig. 5: Phase space distributions under the effect of (a) linear or (b) non-linear forces acting on the beam

Assuming a generic correlation of the type $x' = Cx^n$ and computing the rms emittance according to Eq. (10) we have

$$\varepsilon_{\text{rms}}^2 = C\sqrt{\left\langle x^2 \right\rangle \left\langle x^{2n} \right\rangle - \left\langle x^{n+1} \right\rangle^2} \quad \begin{cases} n = 1 \Rightarrow \varepsilon_{\text{rms}} = 0 \\ n > 1 \Rightarrow \varepsilon_{\text{rms}} \neq 0 \end{cases}. \tag{11}$$

When $n = 1$, the line is straight and the rms emittance is $\varepsilon_{\text{rms}} = 0$. When $n > 1$ the relationship is non-linear, the line in phase space is curved, and the rms emittance is, in general, not zero. Both distributions have zero area. Therefore, we conclude that even when the phase space area is zero, if the distribution is lying on a curved line, its rms emittance is not zero. The rms emittance depends not only on the area occupied by the beam in phase space, but also on distortions produced by non-linear forces.

If the beam is subject to acceleration, it is more convenient to use the rms normalized emittance, for which the transverse momentum $p_x = p_z x' = m_0 c \beta \gamma x'$ is used instead of the divergence:

$$\varepsilon_{n,\text{rms}} = \frac{1}{m_0 c}\sqrt{\sigma_x^2 \sigma_{p_x}^2 - \sigma_{xp_x}^2} = \frac{1}{m_0 c}\sqrt{\left(\left\langle x^2 \right\rangle \left\langle p_x^2 \right\rangle - \left\langle xp_x \right\rangle^2\right)} = \sqrt{\left(\left\langle x^2 \right\rangle \left\langle (\beta\gamma x')^2 \right\rangle - \left\langle x\beta\gamma x' \right\rangle^2\right)}. \tag{12}$$

The reason for introducing a normalized emittance is that the divergences of the particles $x' = p_x/p$ are reduced during acceleration as p increases. Thus, acceleration reduces the un-normalized emittance, but does not affect the normalized emittance. Assuming a small energy spread within the beam, the normalized and un-normalized emittances can be related by the approximated relation $\langle \beta\gamma \rangle \varepsilon_{\text{rms}}$. This approximation, which is often used in conventional accelerators, may be strongly misleading when adopted for describing beams with significant energy spread, like those currently produced by plasma accelerators. A more careful analysis is reported next [8].

When the correlations between the energy and transverse positions are negligible (as in a drift without collective effects), Eq. (12) can be written as

$$\varepsilon_{n,\text{rms}}^2 = \left\langle \beta^2\gamma^2 \right\rangle \left\langle x^2 \right\rangle \left\langle x'^2 \right\rangle - \left\langle \beta\gamma \right\rangle^2 \left\langle xx' \right\rangle^2. \tag{13}$$

Consider now the definition of relative energy spread

$$\sigma_\gamma^2 = \frac{\left\langle \beta^2\gamma^2 \right\rangle - \left\langle \beta\gamma \right\rangle^2}{\left\langle \beta\gamma \right\rangle^2},$$

which can be inserted into Eq. (13) to give

$$\varepsilon_{n,\text{rms}}^2 = \left\langle \beta^2\gamma^2 \right\rangle \sigma_\gamma^2 \left\langle x^2 \right\rangle \left\langle x'^2 \right\rangle + \left\langle \beta\gamma \right\rangle^2 \left(\left\langle x^2 \right\rangle \left\langle x'^2 \right\rangle - \left\langle xx' \right\rangle^2\right). \tag{14}$$

Assuming relativistic particles ($\beta = 1$), we get

$$\varepsilon^2_{n,\mathrm{rms}} = \left\langle \gamma^2 \right\rangle \left(\sigma^2_\gamma \sigma^2_x \sigma^2_{x'} + \varepsilon^2_{\mathrm{rms}} \right). \tag{15}$$

If the first term in the parentheses is negligible, we find the conventional approximation of the normalized emittance, as $\langle \gamma \rangle \varepsilon_{\mathrm{rms}}$. For a conventional accelerator, this might generally be the case. Considering, for example, beam parameters for the SPARC_LAB photoinjector [9]: at 5 MeV the ratio between the first and the second term is $\sim 10^{-3}$; while at 150 MeV it is $\sim 10^{-5}$. Conversely, using typical beam parameters at the plasma–vacuum interface, the first term is of the same order of magnitude as for conventional accelerators at low energies; however, owing to the rapid increase of the bunch size outside the plasma ($\sigma_{x'} \sim$ mrad) and the large energy spread ($\sigma_\gamma > 1\%$), it becomes predominant compared with the second term after a drift of a few millimetres. *Therefore, the use of approximated formulas when measuring the normalized emittance of plasma accelerated particle beams is inappropriate* [10].

4 The root mean square envelope equation

We are now interested in following the evolution of particle distribution during beam transport and acceleration. One can use the first collective variable defined in Eq. (6), the second moment of the distribution termed rms beam envelope, to derive a differential equation suitable for describing the rms beam envelope dynamics [11]. To this end, let us compute the first and second derivative of σ_x [4]:

$$\frac{\mathrm{d}\sigma_x}{\mathrm{d}z} = \frac{\mathrm{d}}{\mathrm{d}z}\sqrt{\left\langle x^2 \right\rangle} = \frac{1}{2\sigma_x}\frac{\mathrm{d}}{\mathrm{d}z}\left\langle x^2 \right\rangle = \frac{1}{2\sigma_x}2\left\langle xx' \right\rangle = \frac{\sigma_{xx'}}{\sigma_x}$$

$$\frac{\mathrm{d}^2\sigma_x}{\mathrm{d}z^2} = \frac{\mathrm{d}}{\mathrm{d}z}\frac{\sigma_{xx'}}{\sigma_x} = \frac{1}{\sigma_x}\frac{\mathrm{d}\sigma_{xx'}}{\mathrm{d}z} - \frac{\sigma^2_{xx'}}{\sigma^3_x} = \frac{1}{\sigma_x}\left(\left\langle x'^2 \right\rangle + \left\langle xx'' \right\rangle\right) - \frac{\sigma^2_{xx'}}{\sigma^3_x} = \frac{\sigma^2_{x'} + \left\langle xx'' \right\rangle}{\sigma_x} - \frac{\sigma^2_{xx'}}{\sigma^3_x} \tag{16}$$

Rearranging the second derivative in Eq. (16), we obtain a second-order non-linear differential equation for the beam envelope evolution,

$$\sigma''_x = \frac{\sigma^2_x \sigma^2_{x'} - \sigma^2_{xx'}}{\sigma^3_x} + \frac{\left\langle xx'' \right\rangle}{\sigma_x}, \tag{17}$$

or, in a more convenient form, using the rms emittance definition Eq. (10),

$$\sigma''_x - \frac{1}{\sigma_x}\left\langle xx'' \right\rangle = \frac{\varepsilon^2_{\mathrm{rms}}}{\sigma^3_x}. \tag{18}$$

In Eq. (18), the emittance term can be interpreted physically as an outward pressure on the beam envelope produced by the rms spread in trajectory angle, which is parameterized by the rms emittance.

Let's now consider, for example, the simple case with $\left\langle xx'' \right\rangle = 0$, describing a beam drifting in free space. The envelope equation reduces to

$$\sigma^3_x \sigma''_x = \varepsilon^2_{\mathrm{rms}}. \tag{19}$$

With initial conditions σ_0, σ'_0 at z_0, depending on the upstream transport channel, Eq. (19) has a hyperbolic solution:

$$\sigma(z) = \sqrt{\left(\sigma_0 + \sigma'_0\left(z - z_0\right)\right)^2 + \frac{\varepsilon^2_{\mathrm{rms}}}{\sigma^2_0}\left(z - z_0\right)^2}. \tag{20}$$

Considering the case of a beam at waist ($\langle \mathbf{xx'} \rangle = \mathbf{0}$) with $\sigma'_0 = 0$, using Eq. (5), the solution Eq.~(20) is often written in terms of the β function as

$$\sigma(z) = \sigma_0 \sqrt{1 + \left(\frac{z - z_0}{\beta_{\mathrm{w}}} \right)^2} \ . \tag{21}$$

This relation indicates that without any external focusing element the beam envelope increases from the beam waist by a factor $\sqrt{2}$ with a characteristic length $\beta_w = \sigma_0^2 / \varepsilon_{\mathrm{rms}}$, as shown in Fig 6.
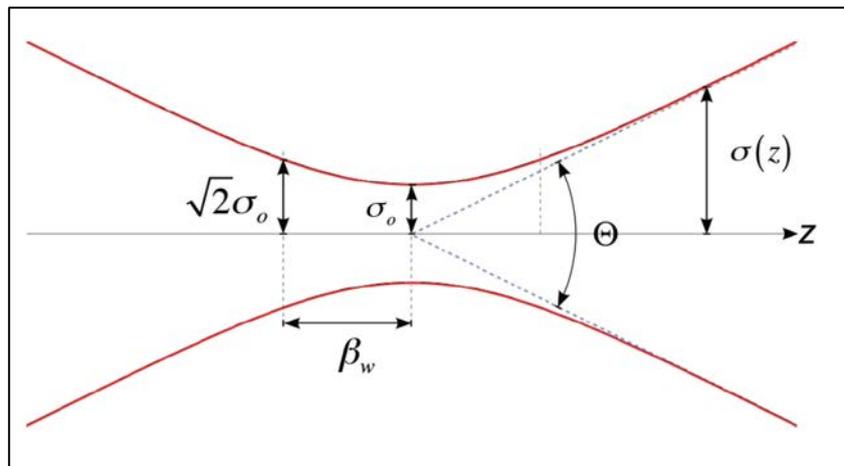

Fig. 6: Schematic representation of the beam envelope behaviour near the beam waist

At the waist, the relation $\varepsilon^2_{\mathrm{rms}} = \sigma^2_{0,x} \sigma^2_{0,x'}$ also holds, which can be inserted into Eq. (20) to give $\sigma^2_x(z) = \sigma^2_{0x'}(z - z_0)^2$. Under this condition, Eq. (15) can be written as

$$\varepsilon^2_{n,\mathrm{rms}}(z) = \langle \gamma^2 \rangle \left(\sigma^2_\gamma \sigma^4_{x'}(z - z_0)^2 + \varepsilon^2_{\mathrm{rms}} \right)$$

showing that beams with large energy spread and divergence undergo a significant normalized emittance growth even in a drift of length $(z - z_0)$ [8, 12].

Notice also that the solution Eq. (21) is exactly analogous to that of a Gaussian light beam for which the beam width $w = 2\sigma_{\mathrm{ph}}$ increases away from its minimum value at the waist w_0 with characteristic length $Z_{\mathrm{R}} = \pi w_0^2 / \lambda$ (Rayleigh length) [4]. This analogy suggests that we can identify an effective emittance of a photon beam as $\varepsilon_{\mathrm{ph}} = \lambda / 4\pi$.

For the effective transport of a beam with finite emittance, it is mandatory to make use of some external force providing beam confinement in the transport or accelerating line. The term $\langle xx'' \rangle$ accounts for external forces when we know x'', given by the single particle equation of motion:

$$\frac{\mathrm{d}p_x}{\mathrm{d}t} = F_x \ . \tag{22}$$

Under the paraxial approximation $p_x \ll p = \beta\gamma mc$, the transverse momentum p_x can be written as $p_x \sim = \sim px' = \beta\gamma m_0 cx'$, so that

$$\frac{\mathrm{d}p_x}{\mathrm{d}t} = \frac{\mathrm{d}}{\mathrm{d}t}(px') = \beta c \frac{\mathrm{d}}{\mathrm{d}z}(px') = F_x \ , \tag{23}$$

and the transverse acceleration results in

$$x'' = -\frac{p'}{p}x' + \frac{F_x}{\beta c p} \quad . \tag{24}$$

It follows that

$$\langle xx'' \rangle = -\frac{p'}{p}\langle xx' \rangle + \frac{\langle xF_x \rangle}{\beta c p} = \frac{p'}{p}\sigma_{xx'} + \frac{\langle xF_x \rangle}{\beta c p} \quad . \tag{25}$$

Inserting Eq. (25) into Eq. (18) and recalling Eq. (16), $\sigma_x' = \sigma_{xx'}/\sigma_x$, the complete rms envelope equation is

$$\sigma_x'' + \frac{p'}{p}\sigma_x' - \frac{1}{\sigma_x}\frac{\langle xF_x \rangle}{\beta c p} = \frac{\varepsilon_{n,\text{rms}}^2}{\gamma^2 \sigma_x^3} \quad , \tag{26}$$

where we have included the normalized emittance $\varepsilon_{n,\text{rms}} = \gamma\varepsilon_{\text{rms}}$. Notice that the effect of longitudinal accelerations appears in the rms envelope equation as an oscillation damping term, called 'adiabatic damping', proportional to p'/p. The term $\langle xF_x \rangle$ represents the moment of any external transverse force acting on the beam, such as that produced by a focusing magnetic channel.

5   External forces

Let's now consider the case of an external linear force acting on the beam in the form $F_x = \mp kx$. It can be focusing or defocusing, according to the sign. The moment of the force is

$$\langle xF_x \rangle = \mp k \langle x^2 \rangle = \mp k\sigma_x^2 \tag{27}$$

and the envelope equation becomes

$$\sigma_x'' + \frac{\gamma'}{\gamma}\sigma_x' \mp k_{\text{ext}}^2\sigma_x = \frac{\varepsilon_{n,\text{rms}}^2}{\gamma^2 \sigma_x^3} \quad , \tag{28}$$

where we have explicitly used the momentum definition $p = \gamma mc$ for a relativistic particle with $\beta \approx 1$ and defined the wavenumber

$$k_{\text{ext}}^2 = \frac{k}{\gamma m_0 c^2} \quad .$$

Typical focusing elements are quadrupoles and solenoids [3]. The magnetic quadrupole field is given in Cartesian coordinates by

$$\begin{cases} B_x = B_0 \dfrac{y}{d} = B_0' y \\[2mm] B_y = B_0 \dfrac{x}{d} = B_0' x \end{cases} , \tag{29}$$

where d is the pole distance and B_0' is the field gradient. The force acting on the beam is $\vec{F}_\perp = qv_z B_0'\left(y\hat{j} - x\hat{i}\right)$ and, when B_0 is positive, is focusing in the x direction and defocusing in the y direction. The focusing strength is

$$k_{\text{quad}} = \frac{qB_0'}{\gamma m_0 c} = k_{\text{ext}}^2 \ .$$

In a solenoid the focusing strength is given by

$$k_{\text{sol}} = \left(\frac{qB_0}{2\gamma m_0 c} \right)^2 = k_{\text{ext}}^2 \ .$$

Notice that the solenoid is always focusing in both directions, an important property when the cylindrical symmetry of the beam must be preserved. However, being a second-order quantity in γ, it is more effective at low energy.

It is interesting to consider the case of a uniform focusing channel without acceleration described by the rms envelope equation

$$\sigma_x'' + k_{\text{ext}}^2 \sigma_x = \frac{\varepsilon_{\text{rms}}^2}{\sigma_x^3} \ . \tag{30}$$

By substituting $\sigma_x = \sqrt{\beta_x \varepsilon_{\text{rms}}}$ into Eq. (30) one obtains an equation for the 'betatron function' $\beta_x(z)$ that is independent of the emittance term:

$$\beta_x'' + 2k_{\text{ext}}^2 \beta_x = \frac{2}{\beta_x} + \frac{\beta_x'^2}{2\beta_x} \ . \tag{31}$$

Equation (31) contains just the transport channel focusing strength and, being independent of the beam parameters, suggests that the meaning of the betatron function is to describe the transport line characteristic by itself. The betatron function reflects exterior forces from focusing magnets, and is highly dependent on the particular arrangement of the quadrupole magnets. The equilibrium, or matched, solution of Eq. (31) is given by

$$\beta_{\text{eq}} = \frac{1}{k_{\text{ext}}} = \frac{\lambda_\beta}{2\pi} \ ,$$

as can be easily verified. This result shows that the matched β_x function is simply the inverse of the focusing wave number or, equivalently, is proportional to the 'betatron wavelength' λ_β.

6   Space charge forces

Another important force acting on the beam is the one produced by the beam itself due to the internal coulomb forces. The net effect of the coulomb interaction in a multiparticle system can be classified into two regimes [3]:

    i)   *collisional regime*, dominated by binary collisions caused by close particle encounters;

    ii) *collective regime* or *space charge regime*, dominated by the self-field produced by the particles' distribution, which varies appreciably only over large distances compared with the average separation of the particles.

A measure for the relative importance of collisional versus collective effects in a beam with particle density *n* is the relativistic *Debye length*,

$$\lambda_{\mathrm{D}} = \sqrt{\frac{\varepsilon_0 \gamma^2 k_{\mathrm{B}} T_{\mathrm{b}}}{e^2 n}} \; , \tag{32}$$

where the transverse beam temperature T_{b} is defined as $k_{\mathrm{B}} T_{\mathrm{b}} = \gamma m_0 \langle v_\perp^2 \rangle$, and k_{B} is the Boltzmann constant. As long as the Debye length remains small compared with the particle bunch transverse size, the beam is in the space charge dominated regime and is not sensitive to binary collisions. Smooth functions for the charge and field distributions can be used in this case, and the space charge force can be treated as an external applied force. The space charge field can be separated into linear and non-linear terms as a function of displacement from the beam axis. The linear space charge term defocuses the beam and leads to an increase in beam size. The non-linear space charge terms also increase the rms emittance by distorting the phase space distribution. Under the paraxial approximation of particle motion, we can consider the linear component alone. We shall see next that the linear component of the space charge field can also induce emittance growth when correlations along the bunch are taken into account.

For a bunched beam of uniform charge distribution in a cylinder of radius R and length L, carrying a current $\hat{I}$ and moving with longitudinal velocity $v_z = \beta c$, the linear component of the longitudinal and transverse space charge field are given approximately by [13]

$$E_z(\zeta) = \frac{\hat{I} L}{2\pi \varepsilon_0 R^2 \beta c} h(\zeta) \; , \tag{33}$$

$$E_{\mathrm{r}}(r, \zeta) = \frac{\hat{I} r}{2\pi \varepsilon_0 R^2 \beta c} g(\zeta) \; . \tag{34}$$

The field form factor is described by the functions

$$h(\zeta) = \sqrt{A + (1-\zeta)^2} - \sqrt{A + \zeta^2 + (2\zeta - 1)} \; , \tag{35}$$

$$g(\zeta) = \frac{(1-\zeta)}{2\sqrt{A^2 + (1-\zeta)^2}} + \frac{\zeta}{2\sqrt{A^2 + \zeta}} \; , \tag{36}$$

where $\zeta = z/L$ is the normalized longitudinal coordinate along the bunch and $A = R/\gamma L$ is the beam aspect ratio. The field form factors account for the variation of the fields along the bunch. As γ increases, $g(\zeta) \to 1$ and $h(\zeta) \to 0$, thus showing that space charge fields mainly affect transverse beam dynamics. It shows also that an energy increase corresponds to a bunch lengthening in the moving frame $L' = \gamma L$, leading to a vanishing longitudinal field component, as in the case of a continuous beam in the laboratory frame.

To evaluate the force acting on the beam, one must also account for the azimuthal magnetic field associated with the beam current, which, in cylindrical symmetry, is given by

$$B_\vartheta = \frac{\beta}{c} E_r .$$

Thus, the Lorentz force acting on each single particle is given by

$$F_r = e(E_r - \beta c B_\vartheta) = e(1 - \beta^2) E_r = \frac{e E_r}{\gamma^2} . \tag{37}$$

The attractive magnetic force, which becomes significant at high velocities, tends to compensate for the repulsive electric force. Therefore, space charge defocusing is primarily a non-relativistic effect and decreases as γ^{-2}.

To include space charge forces in the envelope equation, let us start by writing the space charge forces produced by the previous fields in Cartesian coordinates:

$$F_x = \frac{e\hat{I}x}{2\pi\gamma^2\varepsilon_0\sigma_x^2\beta c}g(\zeta) \ . \tag{38}$$

Then, computing the moment of the force, we need

$$x'' = \frac{F_x}{\beta cp} = \frac{eIx}{2\pi\varepsilon_0\gamma^3 m_0\beta^3 c^3\sigma_x^2} = \frac{k_{sc}(\zeta)}{(\beta\gamma)^3\sigma_x^2} \tag{39}$$

where we have introduced the generalized beam perveance,

$$k_{sc}(\zeta) = \frac{2\hat{I}}{I_A}g(\zeta) \ , \tag{40}$$

normalized to the Alfven current $I_A = 4\pi\varepsilon_0 m_0 c^3/e = 17$ kA for electrons. Notice that in this case the perveance in Eq. (40) explicitly depends on the slice coordinate ζ. We can now calculate the term that enters the envelope equation for a relativistic beam,

$$\langle xx''\rangle = \frac{k_{sc}}{\gamma^3\sigma_x^2}\langle x^2\rangle = \frac{k_{sc}}{\gamma^3} \ , \tag{41}$$

leading to the complete envelope equation

$$\sigma_x'' + \frac{\gamma'}{\gamma}\sigma_x' + k_{ext}^2\sigma_x = \frac{\varepsilon_{n,rms}^2}{\gamma^2\sigma_x^3} + \frac{k_{sc}}{\gamma^3\sigma_x} \ . \tag{42}$$

From the envelope equation Eq. (42), we can identify two regimes of beam propagation: *space charge dominated* and *emittance dominated*. A beam is space charge dominated as long as the space charge collective forces are largely dominant over the emittance pressure. In this regime, the linear component of the space charge force produces a quasi-laminar propagation of the beam, as one can see by integrating one time Eq. (39) under the paraxial ray approximation $x' \ll 1$. A measure of the relative importance of space charge effects versus emittance pressure is given by the *laminarity parameter*, defined as the ratio between the space charge term and the emittance term:

$$\rho = \frac{\hat{I}}{2I_A\gamma}\frac{\sigma^2}{\varepsilon_n^2} \ . \tag{43}$$

When ρ greatly exceeds unity, the beam behaves as a laminar flow (all beam particles move on trajectories that do not cross), and transport and acceleration require a careful tuning of focusing and accelerating elements to keep laminarity. Correlated emittance growth is typical in this regime, which can be made reversible if proper beam matching conditions are fulfilled, as discussed next. When $\rho < 1$, the beam is emittance dominated (thermal regime) and space charge effects can be neglected. The transition to the thermal regime occurs when $\rho \approx 1$, corresponding to the transition energy

$$\gamma_{tr} = \frac{\hat{I}}{2I_A}\frac{\sigma^2}{\varepsilon_n^2} \ . \tag{44}$$

For example, a beam with $\hat{I} = 100$ A, $\varepsilon_n = 1$ µm, and $\sigma = 300$ µm is leaving the space charge dominated regime and is entering the thermal regime at the transition energy of 131 MeV. From this example, one may conclude that the space charge dominated regime is typical of low-energy beams. Actually, for such applications as linac-driven free electron lasers, peak currents exceeding kiloamperes are required. Space charge effects may recur if bunch compressors are active at higher energies and a new energy threshold with higher $\hat{I}$ must be considered.

7 Correlated emittance oscillations

When longitudinal correlations within the bunch are important, like that induced by space charge effects, beam envelope evolution is generally also dependent on the bunch coordinate ζ. In this case, the bunch should be considered as an ensemble of n longitudinal slices of envelope $\sigma_s(z, \zeta)$, whose evolution can be computed from n slice envelope equations equivalent to Eq. (42), provided that the bunch parameters refer to each single slice: γ_s, γ'_s, $k_{sc,s} = k_{sc} g(\zeta)$. Correlations within the bunch may cause emittance oscillations that can be evaluated, once an analytical or numerical solution [13] of the slice envelope equation is known, by using the following correlated emittance definition:

$$\varepsilon_{\text{rms,cor}} = \sqrt{\left\langle \sigma_s^2 \right\rangle \left\langle \sigma_s'^2 \right\rangle - \left\langle \sigma_s \sigma_s' \right\rangle^2} \ , \tag{45}$$

where the average is performed over the entire slice ensemble. In the simplest case of a two-slice model, the previous definition reduces to

$$\varepsilon_{\text{rms,cor}} = \left| \sigma_1 \sigma_2' - \sigma_2 \sigma_1' \right| \ , \tag{46}$$

which represents a simple and useful formula for an estimation of the emittance scaling [14].

The total normalized rms emittance is given by the superposition of the correlated and uncorrelated terms as

$$\varepsilon_{\text{rms,cor}} = \left\langle \gamma \right\rangle \sqrt{\varepsilon_{\text{rms}}^2 + \varepsilon_{\text{rms,cor}}^2} \ . \tag{47}$$

An interesting example to consider here, showing the consequences of non-perfect beam matching, is the propagation of a beam in the space charge dominated regime nearly matched to an external focusing channel ($k_{ext} = k_{sol}$), as illustrated in Fig. 7. To simplify our computations, we can neglect acceleration, as in the case of a simple beam transport line. The envelope equation for each slice, indicated as σ_s, reduces to

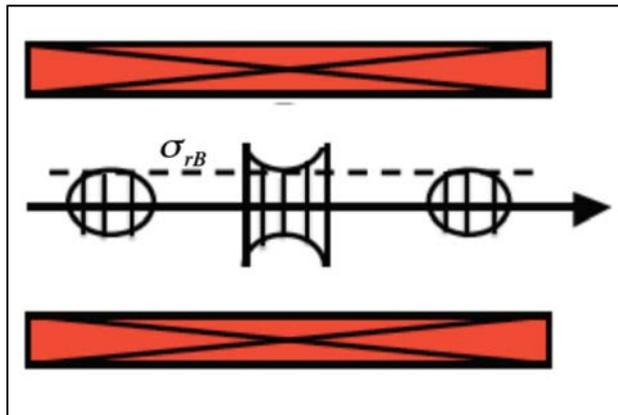$$\sigma_s'' + k_{ext}^2 \sigma_s = \frac{k_{sc,s}}{\gamma^3 \sigma_s} \ . \tag{48}$$

Fig. 7: Schematic representation of a nearly matched beam in a long solenoid. The dashed line represents the reference slice envelope fully matched to the Brillouin flow condition. The other slice envelopes are oscillating around the equilibrium solution.

A stationary solution, called the *Brillouin flow*, is given by

$$\sigma_{s,B} = \frac{1}{k_{ext}^2} \sqrt{\frac{\hat{I} g(\zeta)}{2\gamma^3 I_A}} \ , \tag{49}$$

where the local dependence of the current $\hat{I}_s = \hat{I} g(\zeta)$ within the bunch has been explicitly indicated. This solution represents the matching conditions for which the external focusing completely balances the internal space charge force. Unfortunately, since k_{ext} has a slice-independent constant value, the Brillouin matching condition cannot be achieved at the same time for all of the bunch slices. Assuming that there is a reference slice perfectly matched with an envelope $\sigma_{r,B}$, the matching condition for the other slices can be written as

$$\sigma_{sB} = \sigma_{rB} + \frac{\sigma_{rB}}{2}\left(\frac{\delta I_s}{\hat{I}}\right) \ , \tag{50}$$

with respect to the reference slice. Considering a small perturbation δ_s from the equilibrium in the form

$$\sigma_s = \sigma_{s,B} + \delta_s \ , \tag{51}$$

and substituting into Eq. (48), we can obtain a linearized equation for the slice offset

$$\delta_s'' + 2k_{ext}^2\delta_s = 0 \ , \tag{52}$$

which has a solution given by

$$\delta_s = \delta_0 \cos\left(\sqrt{2}k_{ext}z\right) \ , \tag{53}$$

where $\delta_0 = \sigma - \sigma_{sB}$ is the amplitude of the initial slice mismatch, which we assume, for convenience, is the same for all slices. Inserting Eq. (53) into Eq. (51) we get the perturbed solution:

$$\sigma_s = \sigma_{s,B} + \delta_0 \cos\left(\sqrt{2}k_{ext}z\right). \tag{54}$$

Equation (54) shows that slice envelopes oscillate together around the equilibrium solution with the same frequency for all slices ($\sqrt{2}k_{ext}$, often called the plasma frequency) dependent only on the external focusing forces. This solution represents a collective behaviour of the bunch, similar to that of the electrons subject to the restoring force of ions in a plasma. Using the two-slice model and Eq. (54), the emittance evolution Eq. (46) results in

$$\varepsilon_{\text{rms,cor}} = \frac{1}{4} k_{\text{sol}} \sigma_{\text{rB}} \left| \frac{\Delta I}{\hat{I}} \delta_0 \sin\left(\sqrt{2} k_{\text{ext}} z\right) \right| ,\tag{55}$$

where $\Delta I = \hat{I}_1 - \hat{I}_2$. Notice that, in this simple case, envelope oscillations of the mismatched slices induce correlated emittance oscillations that periodically return to zero, showing the reversible nature of the correlated emittance growth. It is, in fact, the coupling between transverse and longitudinal motion induced by the space charge fields that allows reversibility. With proper tuning of the transport line length or of the focusing field, one can compensate for the transverse emittance growth at the expense of the longitudinal emittance.

At first, it may seem surprising that a beam with a single charge species can exhibit plasma oscillations, which are characteristic of plasmas composed of two-charge species. However, the effect of the external focusing force can play the role of the other charge species, providing the necessary restoring force that is the cause of such collective oscillations, as shown in Fig. 8. The beam can actually be considered as a single-component, relativistic, cold plasma.
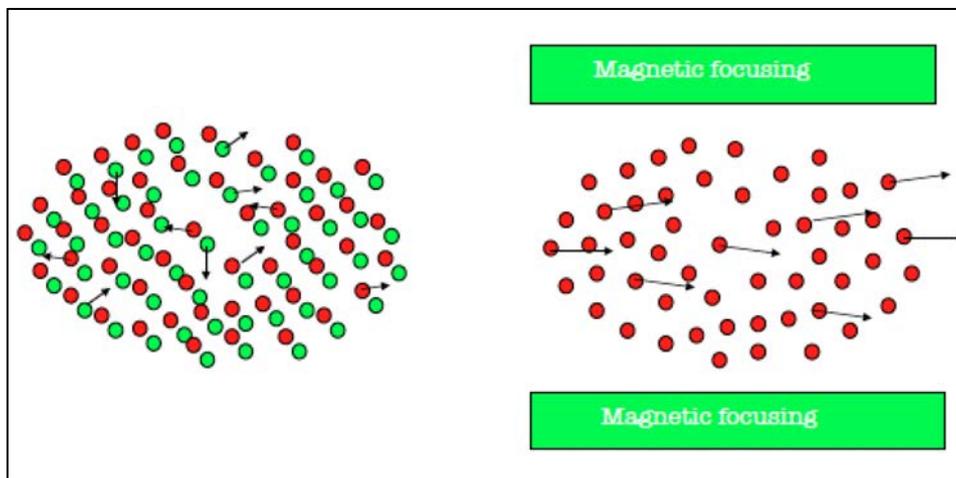

Fig. 8: The restoring force produced by the ions (green dots) in a plasma may cause electron (red dots) oscillations around the equilibrium distribution. In a similar way, the restoring force produced by a magnetic field may cause beam envelope oscillations around the matched envelope equilibrium.

It is important to bear in mind that beams in linacs are also different from plasmas in some important respects [5]. One is that beam transit time through a linac is too short for the beam to reach thermal equilibrium. Also, unlike a plasma, the Debye length of the beam may be larger than, or comparable to, the beam radius, so shielding effects may be incomplete.

Acknowledgements

References

[1] T. Shintake, Review of the worldwide SASE FEL development, Proc. 22nd Particle Accelerator Conf., Albuquerque, NM, 2007 (IEEE, New York, 2007), p. 89.
http://dx.doi.org/10.1109/PAC.2007.4440331

[2] L. Serafini and J.B. Rosenzweig, *Phys. Rev. E* **55** (1997) 7565.
https://doi.org/10.1103/PhysRevE.55.7565

[3] M. Reiser, *Theory and Design of Charged Particle Beams* (Wiley, New York, 1994).
http://dx.doi.org/10.1002/9783527617623

[4] J.B. Rosenzweig, *Fundamentals of Beam Physics* (Oxford University Press, Oxford, 2003).
http://dx.doi.org/10.1093/acprof:oso/9780198525547.001.0001

[5] T. Wangler, *Principles of RF Linear Accelerators* (Wiley, New York, 1998).
http://dx.doi.org/10.1002/9783527618408

[6] S. Humphries, *Charged Particle Beams* (Wiley, New York, 2002).

[7] N. Pichoff, in Proceedings of the CERN Accelerator School: Small Accelerators, Zeegse, the Netherlands, 24 May – 2 June 2005, edited by D. Brandt, CERN-2006-012 (CERN, Geneva, 2006), pp. 145-177. http://dx/doi.org/10.5170/CERN-2006-012.145
http://dx.doi.org/10.5170/CERN-2006-012

[8] M. Migliorati *et al.*, *Phys. Rev. ST Accel. Beams* **16** (2013) 011302.
http://dx.doi.org/10.1103/PhysRevSTAB.16.011302

[9] M. Ferrario *et al.*, *Nucl. Instrum. Methods Phys. Res. B* **309** (2013) 183.
http://dx.doi.org/10.1016/j.nimb.2013.03.049

[10] A. Cianchi *et al.*, *Nucl. Instrum. Methods Phys. Res. A* **720** (2013) 153.
http://dx.doi.org/10.1016/j.nima.2012.12.012

[11] F.J. Sacherer, *IEEE Trans. Nucl. Sci.* **NS-18** (1971) 1105.
http://dx.doi.org/10.1109/TNS.1971.4326293

[12] K. Floettmann, *Phys. Rev. ST Accel. Beams* **6** (2003) 034202.
http://dx.doi.org/10.1103/PhysRevSTAB.6.034202

[13] M. Ferrario *et al.*, *Int. J. Mod. Phys. A* **22** (2007) 4214.
http://dx.doi.org/10.1142/S0217751X07037779

[14] J. Buon, in Proceedings of the CERN Accelerator School: 5th General Accelerator Physics Course, Jyvaskyla, Finland, 7 – 18 September 1992, edited by S. Turner, CERN-1994-001 (CERN, Geneva, 1994), pp. 89-116. http://dx/doi.org/10.5170/CERN-1994-001.89